Prediction Downpull Force on Tunnel Gate with Different Gate Lip Geometry

تنبؤ قوة السحب المسلطة على بوابات نفق السد ذات شفة بأشكال مختلفة

Dr. Rassul M. Almaini[1] Dr. Mustafa T. Al-Kifae[2] Dr. Shaymaa A. M. Alhashimi[3]

الخلاصة :

تتعرض بوابات نفقِ السد 0إلى قوى هايدروستاتيكية وهايدروديناميكية نتيجة لظروفِ التشغيل تحت شروط حدودية مختلفة للتصاريف والمناسيب وفتحات البوابة. من بين هذه القوى قوةُ السحب إلى الأسفل الناتجة عن الفرق بين القوةِ المتجهة إلى الأسفل التي تولدها المياه المتدفقة فوق السطح الأعلى للبوابة خلال منشأ حركة البوابة والقوةَ المتجهةَ للأعلى المسلطة على شفة البوابَة الناتجة عن تدفق المياه تحت البوابة من مقدم النفق صوب المؤخرة. يتطلب تخمين قوة السحب معرفة معاملات الضغط المسلطة على السطح العلوي والسفلي للبوابة (K_T , K_B) التي تعتمد على شكل شفة البوابة ومعدل الجريان المار فوق سطح البوابة. تم تطوير نموذج رياضي ثنائي الأبعاد لتخمين قوة السحب المؤثرة على البوابة باستخدام برنامج يسمى (FLUENT) والذي أعتمد في بنائه على طريقة الحجوم المحددة (Finite Volume) لحل المعادلات الحاكمة Reynolds-averged Navier-Stokes equations. تم تحديد مقدار الاضطراب باستخدام نموذج (k-ε) القياسي جرى تطبيق نموذج المحاكاة هذا على نتائج لنموذج هيدروليكي سابق لدراسة تأثير تسع أشكال لشفة البوابة وبنسب مختلفة لفتحة البوابة على قوة السحب المؤثرة. أوضحت النتائج ان شفة البوابة المائلة ($\theta = 35^o$) تعطي اقل قوة سحب. عولجت البيانات إحصائيا" لتقدير قيمة معامل الضغط السفلي (K_B) لمختلف أشكال شفة البوابة.

Abstract

Vertical lift tunnel gates are subjected to hydrostatic and hydrodynamic forces produced as a result of operating condition over a wide range of partial openings, discharge and heads. Among these forces is the unbalanced vertical hydrodynamic force resulting from the difference between the downward force on the top of gate within the gate shaft and the upward force on the gate bottom, the net resultant of these two forces is termed as a downpull force. The estimation of downpull force requires the determination of the top and bottom pressure coefficient (K_T and K_B) which affected by the geometry of gate bottom and the rate of flow passing over the top surface of gate. A two-dimensional CFD model is applied to predict a downpull coefficient (K_T and K_B) which is named as FLUENT program. The finite volume method is employed on a Reynolds averaged Navier-Stokes equations. The turbulence effects are simulated using the standard (k-ε) model. The simulation model is used for relevant experimental data obtained from hydraulic model tests conducted in laboratory for nine gate lip shape with nine gate openings for each gate lip geometry. The procedure is applied to estimate the pressure coefficients (K_T and K_B) for different gate bottom geometry. The results illustrate that the inclined gate lip shape with angle of ($\theta = 35^o$) given a minimum positive values of downpull force. Also, the downpull coefficient depends mainly on the magnitudes and the distribution of (K_B) for a given value of (b2/b1). A general statistical model is built to predict the bottom pressure coefficient for any gate lip geometry.

Key Word:-Downpull forces, Tunnel gate, Turbulent flow, Numerical modeling, FLUENT

1- Asst. Prof., Civil Engineering Dept., Engineering College, Al-Mustanseryah University.
2- Asst. Prof., Technical College of Baghdad
3- Lecture, Highway and Transportation Dept., Engineering College, Al-Mustanseryah University.

Introduction

Vertical lift gates are among the most widely used high head gates for flow regulation or emergency closure of large outlets and conduit. One type of gates is the tunnel-gate which operates through a gate shaft located within the tunnel conduit. However, it may be subjected to large downpull forces and severe vibration as a result of high speed fluid around the gate lip and low pressure due to suction induced by high momentum fluid downstream of the control section. **Aydin, [2002]**

Downpull forces in vertical lift gates are defined as the unbalanced vertical hydrodynamic forces resulting from the difference between the downward force on the gate top due to flow passing over the top gate surface through the upstream and downstream clearance and the upward force results from pressure exerted on the bottom gate surface by the flow issuing beneath the gate. The net force is termed downpull when it is in the downward direction and uplift when it is in the upward direction. The gate designer is called upon to evolve design of high-head gates to keep the downpull forces as small as is feasible to economize the gate and the hoist costs and to insure proper operation and safety.

Many studies were carried out to estimate the downpull and investigated various some relevant parameters exerted on it. Physical models have been constructed in hydraulic laboratories to study the behavior of hydraulic gate design and estimate downpull coefficient but they are expensive, time-consuming and there are many difficulties associated with scaling effects. Today, with the use of high performance computers and more efficient computation fluid dynamics (CFD) codes, the influence of various geometric and hydraulic parameters on the magnitude and distribution of pressure on top and bottom of vertical lift gate can be investigate numerically in reasonable time and expense. **Ferzieger and peric, [1996].**

Cox et. al., [1960] developed a dimensionless relationship for estimating the hydrodynamic forces depended on the effect of ventilation, geometry of gate bottom and clearance of gate shaft with its effect on the stability of gate.

Naudascher et. al., [1964] presented a one dimensional form that can be used for estimating downpull force acting on high head leaf gate taking into account the effect of flow parameters and boundary geometry on it, as follow:-

$$F_d = (K_T - K_B).\ B.\ d.\ \rho\ (v_j^2/2) \quad \text{..... (1)}$$

$$K_T=(H_t-Y_s)/\ (v_j^2/2g) \quad \text{..... (2)}$$

$$K_B=\iint [(H_i - Y_s) / (v_j^2/2g)]\ dB\ dx \quad \text{..... (3)}$$

$$K = K_T - K_B \quad \text{..... (4)}$$

Where:

F_d: downpull force.
K: downpull coefficient.
K_T: top pressure coefficient.
K_B: bottom pressure coefficient.
B: gate width.
d: gate thickness
ρ: water mass density.
v_j : velocity of the contracted jet issuing from underneath the gate.
g: gravitational acceleration.
H_t: piezometric head on gate top surface.
Y_s: piezometric head in contracted jet.
H_i: piezometric head at a point on the gate bottom.

The model that study of hydraulic downpull on high-head leaf gate for power house was conducted by **Smith, [1964]** using different cases of study. These cases depended on varied of gate lip shapes, gate closure speed, gate slot head wall geometry and discharge rating. The study concluded that the maximum downpull on the moving gate during closure was only 74% of that on

the gate at fixed openings.

Uppal and Paul, [1964] conducted that the maximum downpull acting on gate with concave curvature in the webs of bottom beam is depending on the operating head as follow:-

$F_d=0.0418H^{1.625}$ …… (5)

Where: H : operating head.

General studies were made by **Murray and Simmons, [1966]** to determine design parameters for hydraulic downpull on downstream seal, roller-mounted gates located in entrance transition of large conduits. Data were presented in both dimensional and non-dimensional form on the effects of gate leaf and gate shaft geometry and on air vent size. The data are used to obtain downpull values for the San Luis dam outlet works emergency gates. The results indicated a maximum downpull force about (710 kips) would occur during emergency closure of gates if free discharge conditions occur at the downstream gate frame.

Narasimhan and Bhargava, [1975] presented the factors that the magnitude and character of hydrodynamic force on a gate depended on it. The factors are Froud No., gate opening, the geometric parameters of the gate lip and the skin plate arrangements.

The various forces acting on gate during opening and closing were discussed by **Sagar, [1977]**. He determined the hoist capacity with some accuracy to avoid the risk of non-closure particularly in automatic systems. The downpull forces on gate are predicted as follow:-

$F_d=F_t-F_b$ ……(6)

$F_t=\gamma At(H-v_o^2/2g)$ ……. (7)

$F_b = \gamma\ B\ d\ [Hz – (q^2/2g)\ /y\ (y + d\ \tan\theta)]$ ……...……... (8)

Where:

γ: specific weight of water.

F_t ,F_b : force on the top and bottom of gate respectively.

At: top area of gate exposed to water pressure = $Bd+B' d'$

d: thickness of the gate excluding the downstream skin plate and seal assembly.

B': width of skin plate and seal assembly.

d': thickness of downstream skin plate and seal assembly. $Hz= H - v_o^2/2g$.

v_o^2 : average velocity of the flow in the conduit upstream the gate.

q: discharge of water per unit width of the gate.

y: height of the gate opening.

θ : angle between horizontal and sloping bottom of the gate.

A method for prediction the gate shaft pressure was presented by **Sagar, [1978].** The principle of method based on the velocity head of the jet flowing through the upstream gap which is lost due to sudden expansion within the gate shaft as it moves toward downstream gap.

Sagar, [1979] published two empirical methods for predicted of downpull on vertical lift gate. These methods are downpull coefficient method which based on the data of Frot Randall dam outlet tunnel gate and pressure distribution method that based on estimating the total force acting on the top and bottom surfaces of the gate. It was conducted that these methods are directly applied at the gate with shapes similar to those used in developing the formulae. This formula was examined the geometrical factors influencing on downpull force as follow:-

$F_d = f(y/y_o, H_e, e/d, \theta, b_1/b_2, d/y_o, r/d)$ ...…… (9)

Where: y/y_o: opening ratio.

$(e/d, \theta)$:gate bottom geometry.

b_1/b_2: gap width ratio.

d/y_o: thickness of gate.

r/d: the radius of curvature on the upstream bottom portion of the gate.

The effect of various approach flow conditions upon the downpull, local pressure and the discharge characteristics have been investigated for intake gate by **Thang et. al., [1983].** Specification of turbulent condition near separation points on the gate bottom was detailed by using

a laser Doppler-Anemometry. The study concluded that the variation of downpull and discharge coefficient is influenced by the sensitivity of the separated flow pattern near bluff bodies to free stream turbulence and to changes in the mean flow incidence.

A one dimensional analysis of discharge passing under a tunnel gate and of the hydraulic downpull acting on it is presented by **Naudascher et. al., [1986].** It is shown that the downpull is significantly affected not only by the geometry of the gate bottom but also by the rate of flow passing over the top of gate through the gate shaft.

Alkadi, [1997] estimating the downpull force on tunnel gate depending on the top and bottom pressure coefficients. A one dimensional analysis is used to predict the discharge passing over the top of gate, total discharge; top pressure coefficient and the flow condition downstream the gate. The results are verified by comparing with observed measurements. The bottom pressure coefficients have been estimated by prediction the mean pressure and the velocity distribution along the gate bottom using finite element models with constant eddy viscosity and with variable eddy viscosity to facilitate prediction the negative downpull for cases of large gate openings.

Ahmed, [1999] constructed an arbitrary hydraulic model to investigate the effect of fourteen gate lip shapes on the value of downpull force. The study included the investigation of effect of gap width ratio and gate lip geometry on the magnitude of top pressure coefficient. The results indicate that the top pressure coefficient is sensitive to the change in gap width ratio but not changes with gate lip geometry. On the other hand, the bottom pressure coefficient is influenced effectively by the gate lip geometry.

Sagar, [2000] discussed the influence of the gate lip geometry on the hydraulic aspects of cavitations, vibration, downpull and uplift individually. He concluded that the correct choice of gate lip angles required to minimize vibrations and cavitations are much than required for substantial reduction in downpull forces.

Drobir et. al., [2001] investigated the effect of downpull on tunnel type high head gate using a hydraulic model. The model measurements were carried out for particular head water and tail water conditions. According to the tail water conditions free surface flow and submerged flow have occurred. For free surface flow the resulting downpull force of hydraulic model test are compared with the results from calculation according to the method of **Naudascher, [1991].**

A numerical analysis has been developed by **Andrade and Amorim, [2003]** for calculating viscous flows controlled by a vertical lift gate and hydrodynamic forces acting on it. The numerical solution is obtained from the incompressible Navier-Stokes equations. The numerical technique is based on a finite element method. Turbulence effects are simulated by using (k-ε) turbulence model. The model is applied on a vertical lift gate operating in a CESP installation and the results compared with available experimental data at various opening positions.

The foregoing literatures on hydraulic gate reveal that there is not found numerical solution to predict the pressure on the gate within the gate shaft and the distribution of pressure along the gate bottom at the same time. This is necessary for estimating the top and bottom pressure coefficients (K_T & K_B). In the current study an attempt has been to model fluid flow controlled by vertical lift gate using Fluent software and applied on a hydraulic model conducted by **Ahmed, [1999].**

Experimental Investigation

The case study used in this work is the experimental hydraulic model which presented by **Ahmed, [1999].** The model was conducted in rectangular recirculating flume, 4m long, 0.2m wide and 0.3m deep with horizontal steel floor. The flume was covered along its upper part by a thick plate representing the tunnel roof as shown in Fig. (1).

The gate shaft (0.3 * 0.15 * 0.9) m was installed at mid way along the flume; it was made by steel and covered by the plate. The model gate made by a thick plate with thickness of (50mm) was supported by steel frame slide in vertical way of the gate shaft and it can be adjustable by a screw placed on the top cover of the shaft to control the gate openings. The exchangeable bottom plates of

the gate made by steel blocks formed 9 different shapes of gate lip as shown in Fig. (2), each of them was provided with two sets of tap located along the lip parallel to the direction of flow. The procedure which adopted in measurements of each run are as followed:

1- Upstream and downstream piezometric head (Hu&Hd) are measured by using two metric scaled piezometers fixed on the plate of tunnel one at upsteam and the other at downstream of the gate shaft.
2- The piezometer heads on the gate top surface (H_T) were measured using U-shape piezometer installed on the gate top surface then connected to the manometer board through plastic tube.
3- The distribution of piezometer head (H_i) along the gate lip was measured at the point with piezometric holes located in the bottom surface of the gate.
4- The measurement of velocity profiles was made in two stations located at 1.0 and 0.25 m upstream the gate shaft. The current meter was installed at first station to measure velocity profile. The velocity distribution has also been measured using a pitot tubes with a right angle bend of 2mm diameter installed at the second station.

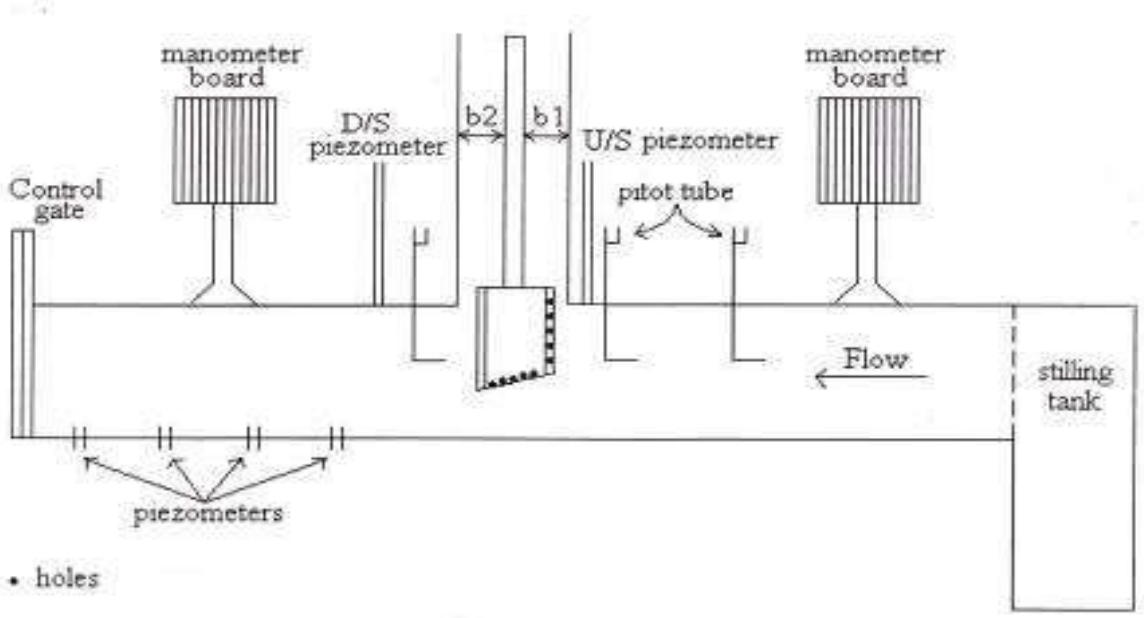

Figure (1):- Tunnel Model under Operation. **[After Ahmed, 1999]**

Numerical Model Description

Fluent is the CFD solver for choice for complex ranging from incompressible to highly compressible flows. It allows you to accurately predict laminar and turbulent flows, various modes of heat transfer, multiphase flows, and other phenomena with complete mesh flexibility and solution-based mesh adoption, **Fluent User's Manual**, **[2003].**

Fluent solves governing equation sequentially using the control volume method. The governing equations are integrated over each control volume to construct discrete algebraic equations for dependent variables. These discrete equations are linearized using an implicit method. As the governing equations are nonlinear and coupled, iteration are needed to achieve a converged solution.

Turbulent flows can be simulated in Fluent using standard (k-ε), LES, RNG, or Reynolds-stress (RSM) closure schemes. The model optimizes computational efficiency by allowing the user to choose between (Second-order upwind, third order and Quick) discretization scheme. The under-relaxation factors are chosen between 0.2 and 0.5.

Turbulent stresses in Reynolds-averaged Navier Stokes equations can be closed using any of several exiting turbulence models. The simple and most widely used two-equation turbulent model

is (k-ε) model that solves two separate equations to allow the turbulent kinetic energy and dissipation rate to be independently determined **Ferzieger and peric, [1996].**

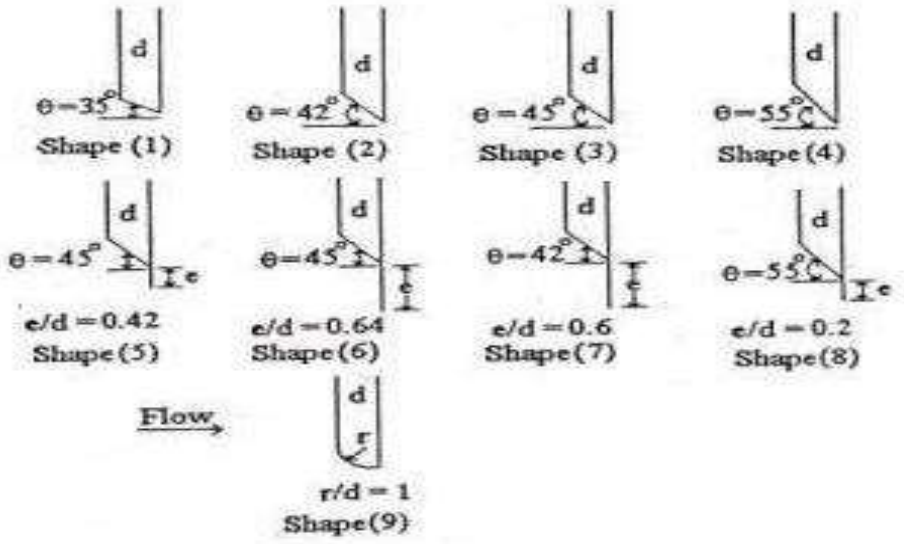

Figure (2):- Gate Lip Shapes. **[After Ahmed, 1999]**

The turbulent kinetic energy, k, is modeled as,

$$\frac{\partial uk}{\partial x}+\frac{\partial vk}{\partial y}=\frac{\partial}{\partial x}\left((\upsilon+\frac{\upsilon_t}{\sigma_k})\frac{\partial k}{\partial x}\right)+\frac{\partial}{\partial y}\left((\upsilon+\frac{\upsilon_t}{\sigma_k})\frac{\partial k}{\partial y}\right)+G-\varepsilon \quad \text{.....(10)}$$

The dissipation rate of k is denoted, ε, and modeled as

$$\frac{\partial u\varepsilon}{\partial x}+\frac{\partial v\varepsilon}{\partial y}=\frac{\partial}{\partial x}\left((\upsilon+\frac{\upsilon_t}{\sigma_\varepsilon})\frac{\partial \varepsilon}{\partial x}\right)+\frac{\partial}{\partial y}\left((\upsilon+\frac{\upsilon_t}{\sigma_\varepsilon})\frac{\partial \varepsilon}{\partial y}\right)+C_1\frac{\varepsilon}{k}G-C_2\frac{\varepsilon^2}{k} \quad \text{.....(11)}$$

The term G, representing the production of turbulent kinetic energy, is modeled identically for the standard, RNG, and realizable (k-ε) models. From the exact equation for the transport of k, this term may be defined as:

$$G=-\rho\,\overline{u_i'u_j'}\frac{\partial u_i}{\partial x_j}=\left[\mu_t\frac{\partial u_i}{\partial x_j}\left(\frac{\partial u_i}{\partial x_j}+\frac{\partial u_j}{\partial x_i}\right)\right] \quad \text{.....(12)}$$

The "eddy" or turbulent viscosity, μ_t, is computed by combining k and ε as follows:

$$\mu_t=C_\mu\,\rho\frac{k^2}{\varepsilon} \quad \text{.....(13)}$$

We used second order upwind discritization scheme for momentum, turbulent kinetic energy and turbulent dissipation rate. Body force weighted discretization scheme will be used for pressure and SIMPLE algorithm for pressure velocity coupling method. Also, the standard (k-ε) model have used in the present study to simulate the effect of turbulence.

Governing Equation

The two dimensional CFD modeling is used to solve a steady state incompressible Reynold-averaged Navier Stokes equations with (k-ε) turbulence closure model which is expressed as **Douglas and Matthews, [1996];**

$$Uj\frac{\partial Ui}{\partial x_j}=\frac{1}{\rho}\frac{\partial p}{\partial x_j}+\frac{\partial}{\partial x_j}\left(\upsilon_e\frac{\partial u_i}{\partial x_j}\right)+\frac{\partial}{\partial x_j}\left(\upsilon_e\frac{\partial u_j}{\partial x_i}\right)+\frac{F_i}{\rho} \quad \text{.....(14)}$$

The 2-D continuity equation for incompressible fluid of steady flow can be expressed as:

$$\frac{\partial u}{\partial x}+\frac{\partial v}{\partial y}=0 \qquad \text{.....(15)}$$

Equation (14) with continuity Eq. (15) completes the set of equations necessary to predict the turbulent flow, always providing that the eddy viscosity is evaluated.

The finite volume method is used in this study which uses a control-volume-based technique to convert the governing equations to algebraic equations that can be solved numerically. This control volume technique consists of integrating the governing equations about each control volume, yielding discrete equations that conserve each quantity on a control-volume basis.

Discretization of the governing equations can be illustrated most easily by considering the steady-state conservation equation for transport of a scalar quantity ϕ , **Hoffmann [1989],** as:

$$\frac{\partial}{\partial x_m}(\rho \phi u_m)=\frac{\partial}{\partial x_m}(\Gamma_\phi \frac{\partial \phi}{\partial x_m})+S_\phi \qquad \text{..... (16)}$$

This equation is demonstrated by the following equation written in integral form for an arbitrary control volume V as follows:

$$\oint \rho \phi \, u_m \, . dA=\oint \Gamma_\phi \nabla_\phi \, . dA+\oint S_\phi \, . dV \qquad \text{..... (17)}$$

Where:

ρ = density , u = velocity vector

A = surface area vector

Γ_ϕ = diffusion coefficient for ϕ

∇_ϕ = gradient of ϕ, and S_ϕ = source of ϕ per unit volume

Equation (17) is applied to each control volume, or cell, in the computational domain. The two-dimensional, quadrilateral cell is an example of such a control volume which is used in this work as shown in Fig.(3). Discretization of Eq. (17) on a given cell yields:

$$\sum_f^{N_{faces}} u_f \, \phi_f A_f = \sum_f^{N_{faces}} \Gamma_\phi (\nabla_\phi)_n A_f + S_\phi V \qquad \text{..... (18)}$$

Where:

N_{faces} = number of faces enclosing cell , ϕ_f = value of f convected through face f

u_f = mass flux through the face , A_f = area of face f

$(\nabla_\phi)_n$ = magnitude of (∇_ϕ) normal to face f and V = cell volume

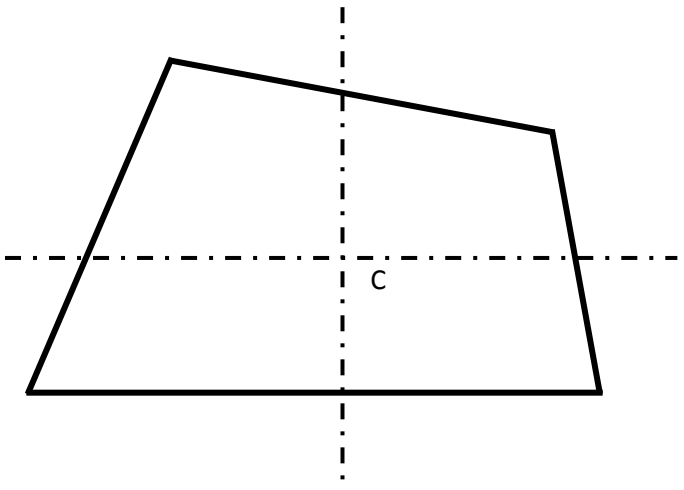

Figure (3):- Control Volume Used to Illustrate Discretization of a Scalar Transport Equation

Boundary Conditions

Appropriate condition must be specified at domain boundaries depending on the nature of the flow. In the simulation performed in the present study, velocity inlet boundary condition is specified. The distribution of velocity inlet values is taken from experimental study and entered to the velocity inlet panel as a profile file. Outlet pressure is used to define outlet boundary conditions. The other faces of the problem domain are defined as a wall. The interior cell zones are defined as a fluid and the faces of gate are taken to be interior wall boundaries.

It is also important to establish grid independent results have been obtained. The grid structure must be fine enough near the gate which is the region of rapid variation. Various flow computational trials have been carried out with different number of grids in x and y directions. The mesh with 2D quadrilateral cells, created by using GAMBIT model as shown in Fig. (4), is used in this study. This mesh then would be exported to FLUENT in order to be used in the solution.

Results and discussion

The downpull coefficient can be estimated from the determining of top and bottom pressure coefficients. The values of (K_T and K_B) are determined for nine different gate lip geometries at various gate openings for each gate lip geometry.

The distribution of pressure head (H_T) on the top surface of the gate is approximately constant as observed from the results of model and as conducted by **Ahmed, [1999],** so the top pressure coefficient (K_T) can be computed as expressed in Eq. (3). The calculation of (K_T) from Eq. (3) is depended on the determination of mean pressure head at the top surface of the gate, the pressure head downstream the gate at contracted jet and the mean jet velocity below the gate. These parameters that needed to predict (K_T) would be obtained from the results of the model. The relation between (K_T) and gate openings (Y/Yo) for different gate lip geometries is indicated in Fig. (5) to observe the effect of gate lip geometries on the value of (K_T). It can be seen from this figure that the gate lip geometry has no significant effect on (K_T) values.

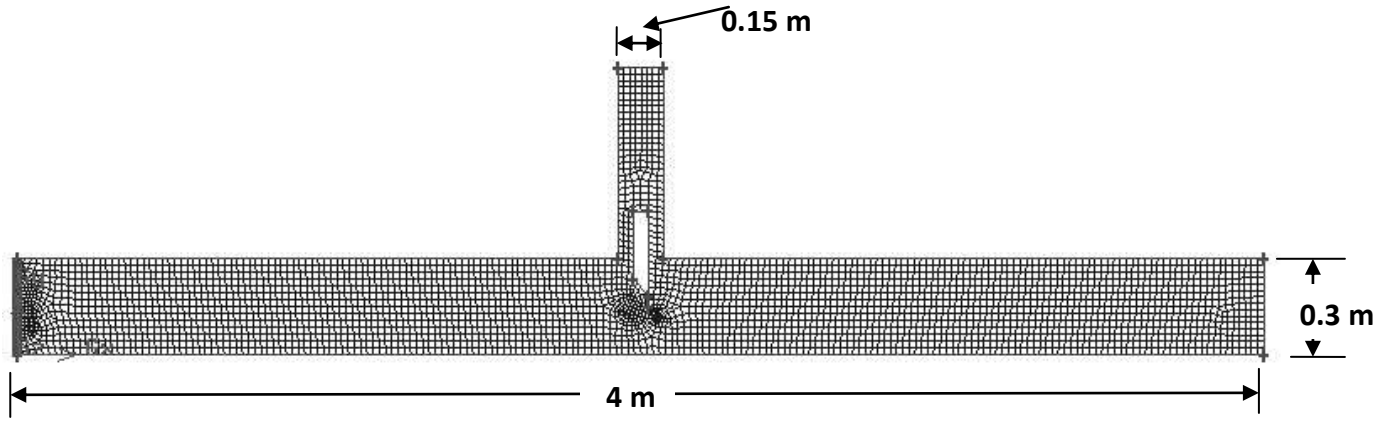

Figure (4):- Mesh Generation Using GAMBIT Model

The bottom pressure coefficient along the gate width can be computed as defined in Eq. (4) by predicting the local pressure head at specific points on the bottom surface of gate (H_i), the pressure head downstream the gate at contracted jet and the mean jet velocity below the gate which are obtained from the results of model. This means that (K_B) is a function of the gate geometry (e/d, r/d, θ) and the geometry of the bounding stream lines (Y/Yo).

The variation of pressure along the bottom of gate is presented as nondimensional plots of (K_B) versus the distance along the gate thickness (x/d) for various gate opening and different gate lip shapes in figs. (6) to (14). The distance x is measured horizontally from the leading edge of the gate

lip toward trailing edge of gate.

The basic objective of prediction (K_B) at various points along the bottom surface of gate is to understand and analyze the flow pattern under the gate and to correlate it with the fluctuating pressure on the gate bottom. Thus, the observation of the separation and reattachment points along the gate lip are useful in the present investigation due to their importance in describing the behavior of the flow beneath the gate and hence to reveal whether the separated flow from the leading edge of the gate lip will reattach or remain separated from the gate bottom. The location of reattachment zone is indicated by a sudden increase in (K_B) followed by a maximal positive pressure whereas the separation zone can be pointed as a region of low constant pressure head followed by sudden rise in pressure. The fact that (K_B) remains particularly constant over the gate thickness indicates that the flow is completely separated from the gate bottom surface, **Reynolds, [1974].**

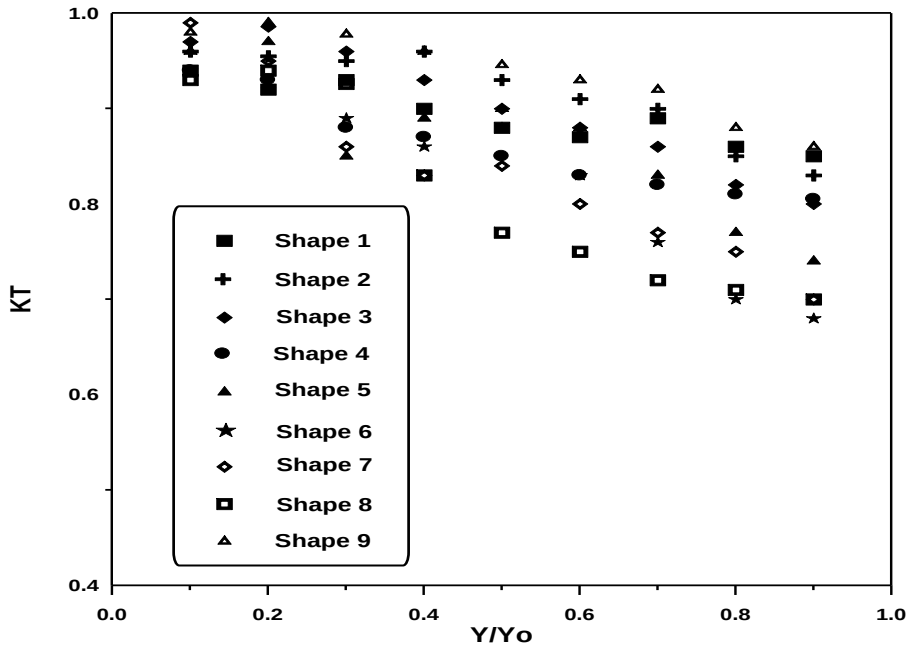

Figure (5):- Variation of Top Pressure Coefficient with Gate Opening (Y/Yo) for Different Gate Lip Geometries

Different gate lip inclination shapes are presented in Figs. (6) to (9) to represent the distribution of bottom pressure coefficient (K_B) along the gate bottom surface. These figures indicate that the over all trend of the distribution profiles moves from relatively high values of (K_B) at the leading edge to slightly smaller values toward the trailing edge of gate (for gate lip of $\theta = 42^o$ and $\theta = 45^o$) as it is obvious from figs. (7) and (8). Such a variation is indicative that there is approximately no flow separation at the leading edge of the gate in these geometries.

Fig. (6) with ($\theta = 35^o$), indicates that the values of (K_B) are high and vary smoothly along the gate lip for opening ratio of (Y/Yo = 10 %). The flow for all remaining gate opening would attach the gate lip from the leading edge to (x/d = 0.57) then separates at (x/d = 0.68) and belong to reattach at the trailing edge of gate. Also, it can be observed from figure that the values of (K_B) are positive except for (Y/Yo = 40%, 50% and 90% at x/d = 0.72).

Fig. (7), for gate lip inclination of ($\theta = 42^o$), shown that the complete attachment is occurred from the leading edge to the trailing edge of the gate bottom surface for gate opening of (Y/Yo = 50%). Also, the flow is attached with gate bottom surface from the leading edge to (x/d = 0.63) for gate opening of (Y/Yo = 20%, 30% and 40%). For other gate openings, the flow is attached at the leading edge of gate bottom with values of (K_B) between 0.85 and 0.75 and then decreased to about 0.67 with smooth variation toward the trailing edge of gate.

Fig. (8), for 45^o sloping lip, indicates that the flow is attached to the bottom surface of gate from

its leading edge up to the (x/d = 0.5), then it is followed by slight instabilities up to the trailing edge. For gate openings (Y/Yo = 70% and 80%), the flow attachment is continued to a point of (x/d = 0.73). From these results can be concluded that the tendency of flow toward separation is reduces by using this shape of gate lip geometry. Furthermore, the figure shown that all values of (K_B) are positive and reduce with small variation toward the trailing edge of gate. Therefore, as the values of (K_B) are high and positive the resulting downpull will be minimized along the entire lip of gate geometry.

Fig.(9) with gate lip angle of 55^o, shows that the flow is attached to the leading edge of gate up to (x/d = 0.11)and then it is separated to reattach again at (x/d = 0.42) for all ratio of gate openings. Also, it can be seen that the values of (K_B) are high and vary smoothly along the gate lip for gate openings of (Y/Yo = 20%).

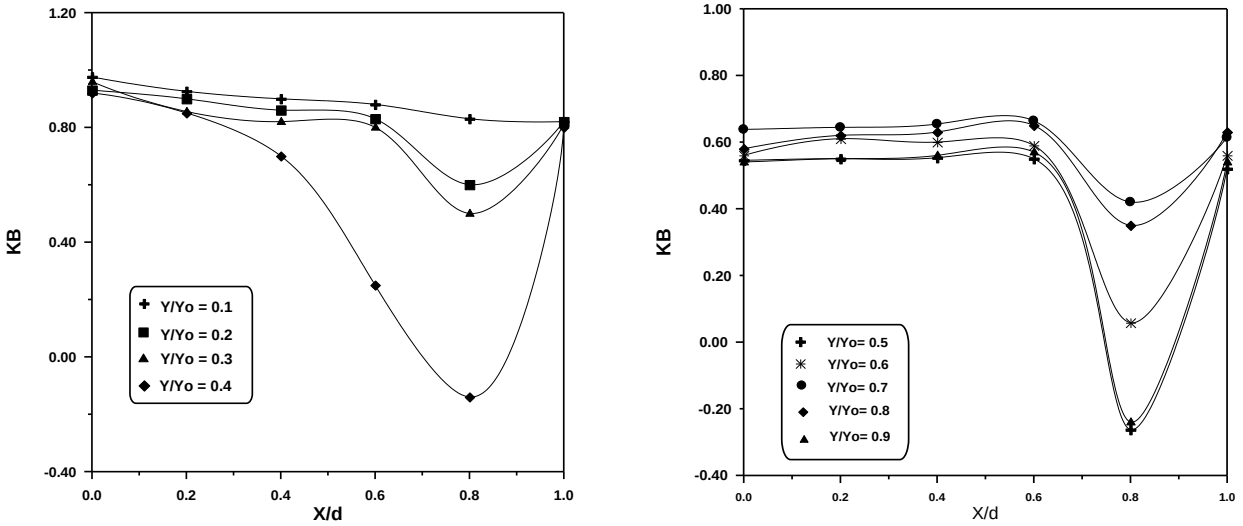

Figure (6):- Variation of the Local Piezometric Head Coefficient over the Gate Bottom for Different Gate Opening. (Shape No. 1)

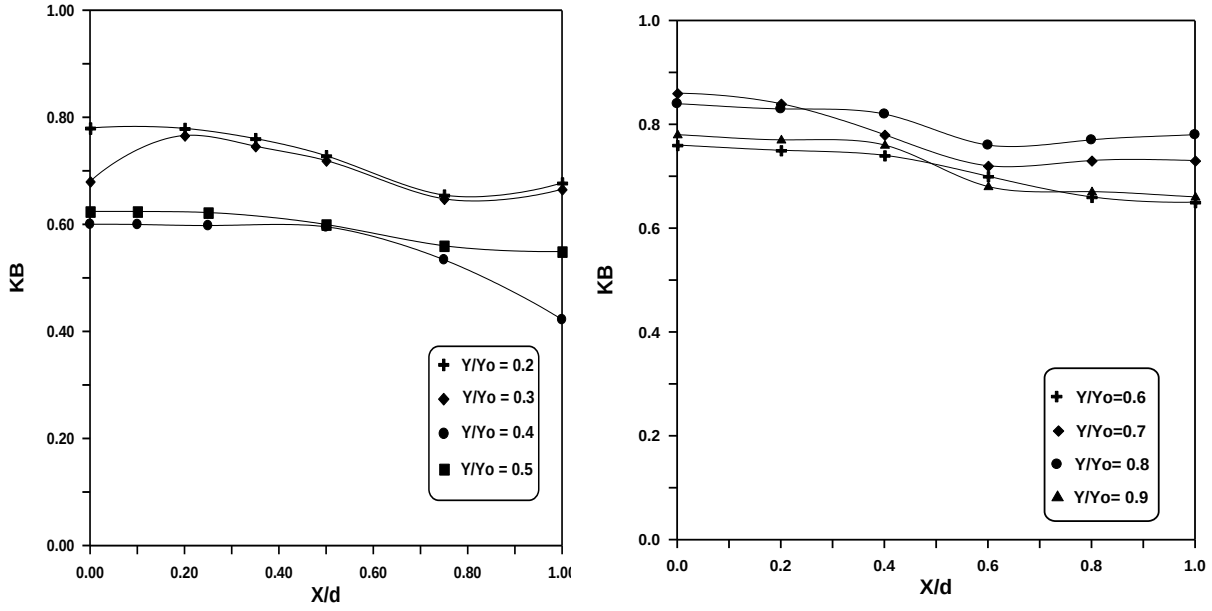

Figure (7):- Variation of the Local Piezometric Head Coefficient over the Gate Bottom for Different Gate Opening. (Shape No. 2)

Figures (10) to (13) present the distribution of (K_B) values on gate bottom surface along inclined gate lips with extensions at the trailing edge of gate. It can be seen from these figures that the using of lip extension provides a stabilizing influence on the distribution of (K_B) along the bottom surface of gate. The values of (K_B) are constant or vary smoothly with values range between (0.7 to 1.0). The gate opening value (Y) in the case of gate with lip extension is measured as a distance from the bottom edge of extension to the tunnel floor.

Fig. (10) indicates the results of gate lip inclination ($\theta = 45^o$) with lip extension (e/d = 0.42). The figure shows that the distribution of (K_B) value along the gate bottom is uniform for all gate openings ratio which representing a stability of gate for this range of openings. Also, it can be seen from this figure that the values of (K_B) are high and may lead to reduce the downpull force to very low value.

Fig. (11) with ($\theta = 45^o$, e/d = 0.64), indicates that the values of (K_B) are approximately constant along the bottom gate surface for openings ratio of (Y/Yo = 10%, 30% and 50%) whereas for the other gate openings ratio the values of (K_B) are vary smoothly from the leading edge to the trailing edge of the bottom surface of gate.

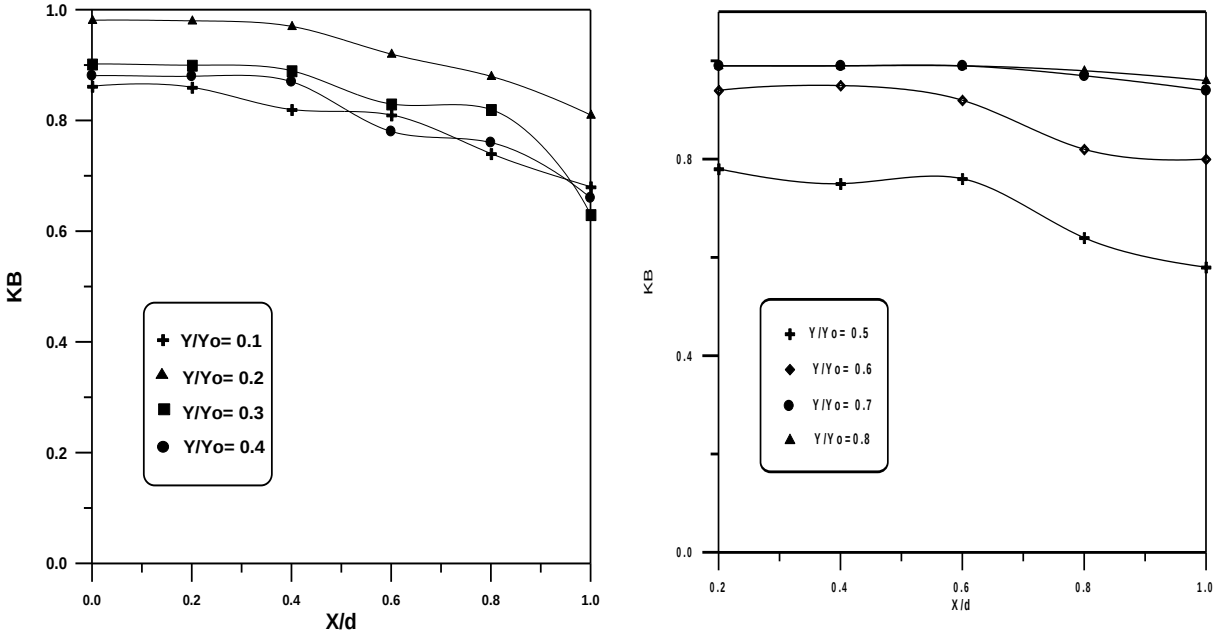

Figure (8):- Variation of the Local Piezometric Head Coefficient over the Gate Bottom for Different Gate Opening. (Shape No. 3)

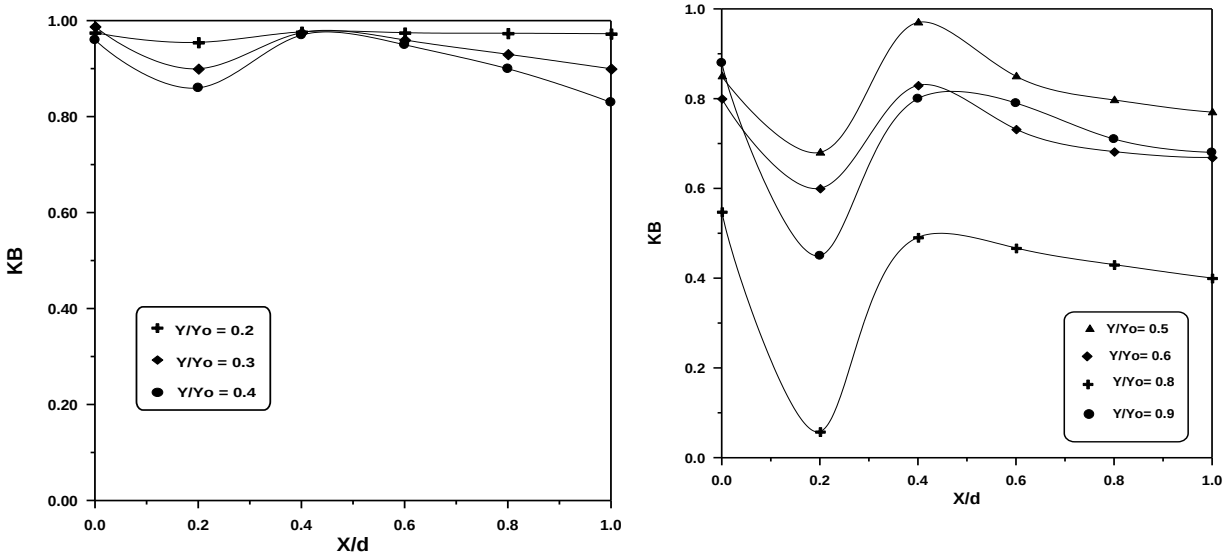

Figure (9):- Variation of the Local Piezometric Head Coefficient over the Gate Bottom for Different Gate Opening. (Shape No. 4)

Fig. (10) indicates the results of gate lip inclination ($\theta = 45^o$) with lip extension (e/d = 0.42). The figure shows that the distribution of (K_B) value along the gate bottom is uniform for all gate openings ratio which representing a stability of gate for this range of openings. Also, it can be seen from this figure that the values of (K_B) are high and may lead to reduce the downpull force to very low value.

Fig. (11) with ($\theta = 45^o$, e/d = 0.64), indicates that the values of (K_B) are approximately constant along the bottom gate surface for openings ratio of (Y/Yo = 10%, 30% and 50%) whereas for the other gate openings ratio the values of (K_B) are vary smoothly from the leading edge to the trailing edge of the bottom surface of gate.

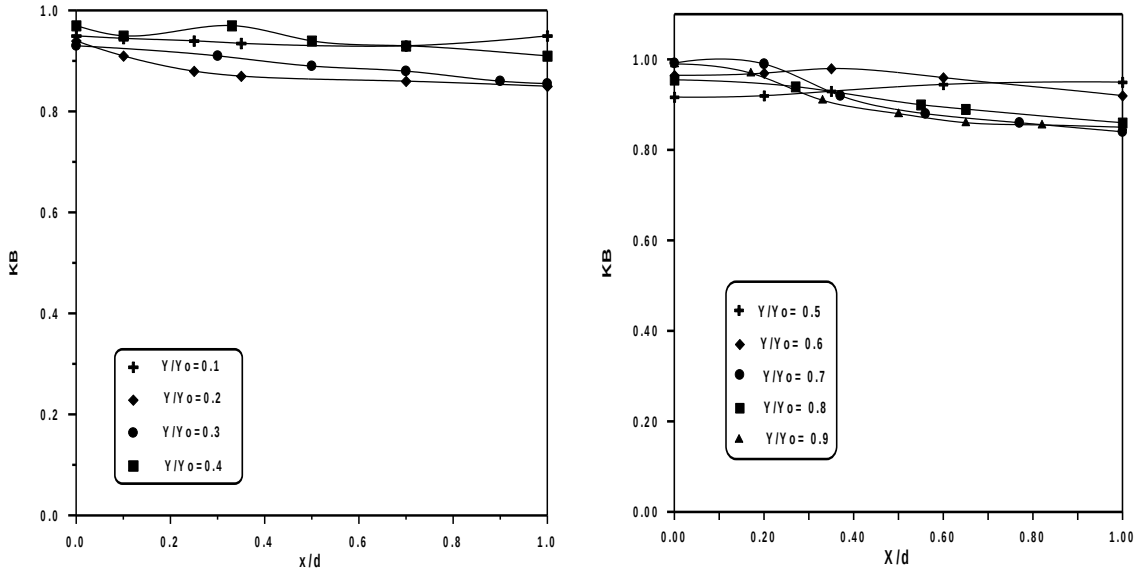

Figure (10):- Variation of the Local Piezometric Head Coefficient over the Gate Bottom for Different Gate Opening. (Shape No. 5)

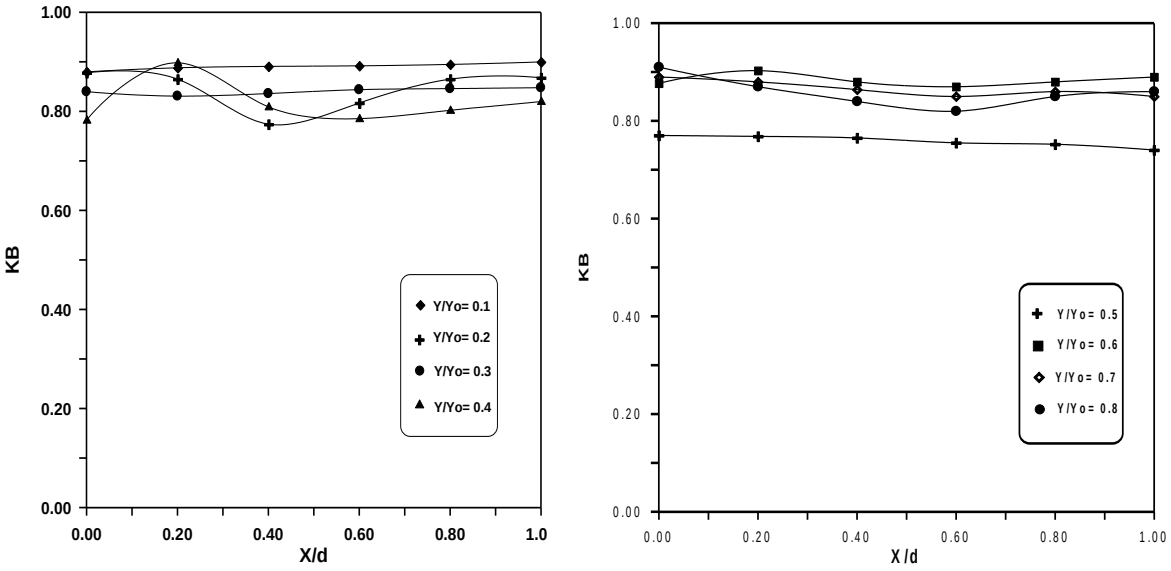

Figure (11):- Variation of the Local Piezometric Head Coefficient over the Gate Bottom for Different Gate Opening. (Shape No. 6)

Fig. (12) for gate lip geometry of ($\theta = 42^o$, e/d = 0.6), shows that distribution of (K_B) is uniform with nearly constant values along the bottom surface of gate for openings ratio between (Y/Yo = 10% to 50%). For the remaining opening ratio of gate can be seen that the flow separates at position of (x/d = 0.32 and 0.69) and the values of (K_B) range from 0.7 to 0.9.

Fig. (13) presents the results of gate lip shape with ($\theta = 55^o$, e/d = 0.2). This figure indicates that the values of (K_B) is approximately constant with small variation along the bottom surface of gate for openings ratio from (Y/Yo = 10%) up to ratio (Y/Yo = 70%). For ratio of (Y/Yo = 80% and 90%), the flow separation occurs at position of (x/d = 0.69) and then reattaches at the trailing edge of gate.

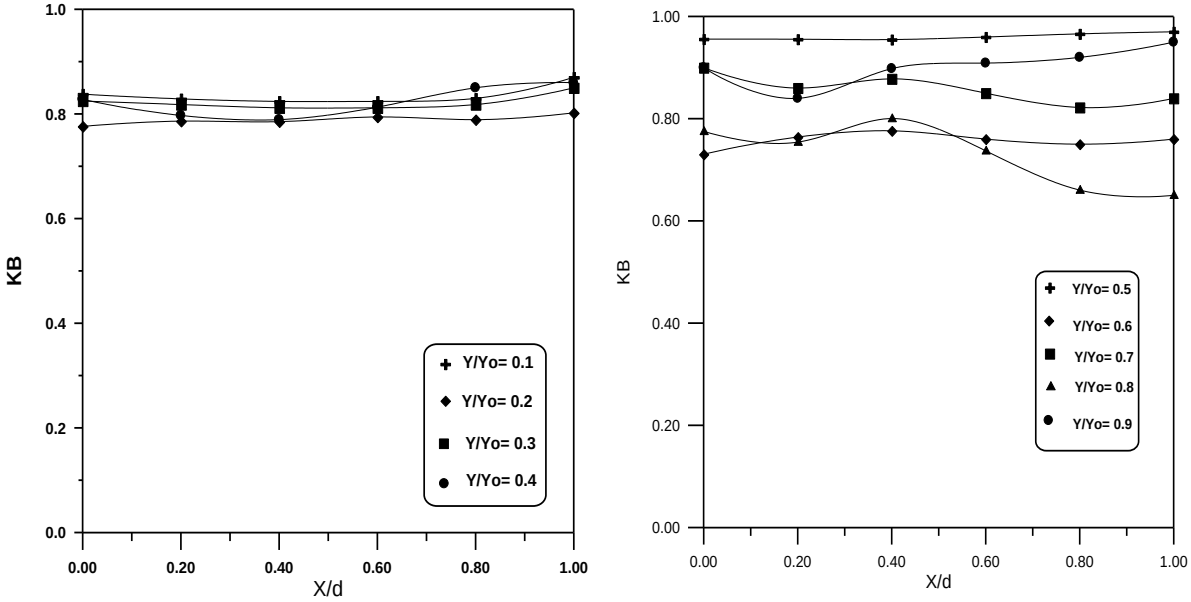

Figure (12):- Variation of the Local Piezometric Head Coefficient over the Gate Bottom for Different Gate Opening. (Shape No.7)

Fig. (14) is drawn to investigate the influence of rounded edge of gate lip with (r/d = 1) on the distribution of pressure head along the bottom surface of gate. This figure indicates that the value of (K_B) is dropped from (1.0 to - 0.3) for gate openings between (Y/Yo = 20% to 40%) whereas for the remaining openings ratio the value of (K_B) is decreased from (1.0) at leading edge to the value of (0.5- 0.03) at the location of (x/d = 0.51) and then continued at the same level with small variation toward the trailing edge of gate.

As mentioned before, the downpull coefficient can be estimated from Eq. (4). The values of (K_T and K_B) are determined for nine different gate lip shapes at various gate openings for each gate lip shape. Therefore, to evaluate the total hydraulic downpull on each shape of gate, the mean values of bottom pressure coefficient (K_B) along the gate surface should be determined for each gate opening ratio.

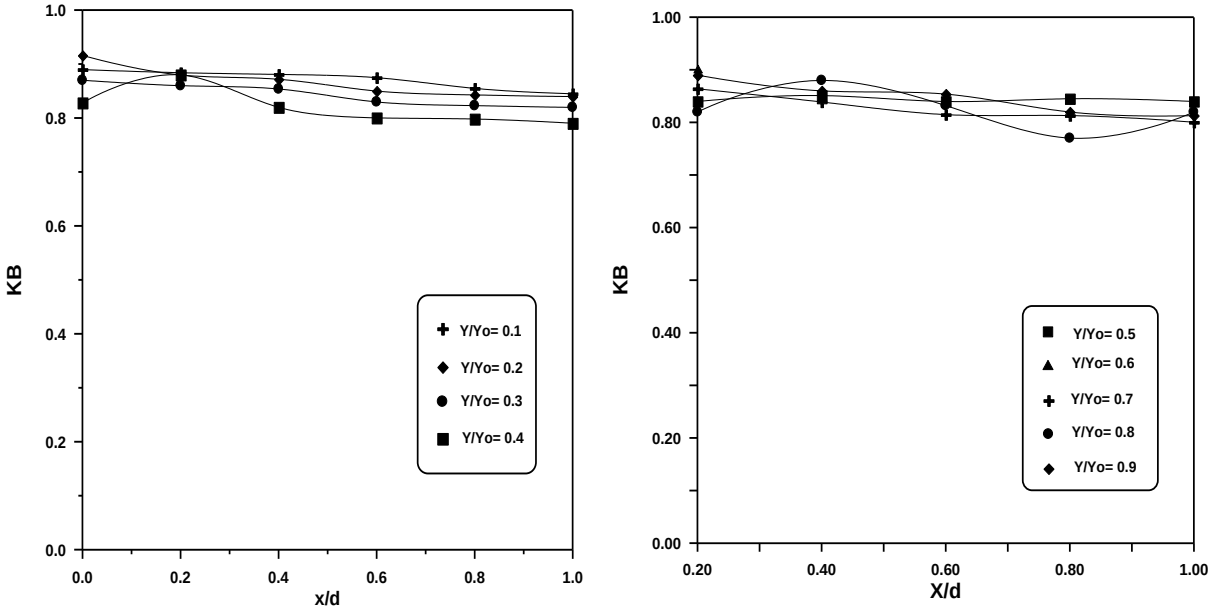

Figure (13):- Variation of the Local Piezometric Head Coefficient over the Gate Bottom for Different Gate Opening. (Shape No. 8)

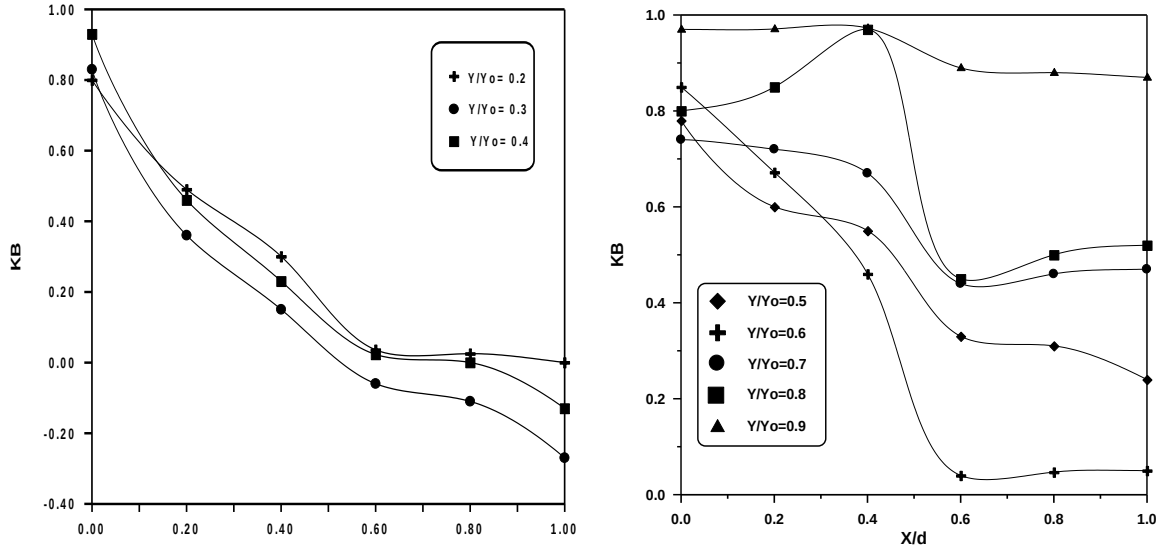

Figure (6-12):- Variation of the Local Piezometric Head Coefficient over the Gate Bottom for Different Gate Opening. (Shape No. 9)

The top pressure coefficient is also determined for each gate opening ratio for all gate geometry. Then the downpull coefficient for each gate lip can be estimated from eq. (4) as shown in Fig. (15). These figure present the value of (K) for nine gate lip shape with gate openings ratio to facilitate the comparison between these values for each gate lip shapes and examine its affect of gate lip shape on the downpull coefficient.

From the previous figures can be concluded that the bottom pressure coefficient is depended mainly on the gate lip geometry but the top pressure coefficient is independed with gate geometry and remain nearly constant for each gap width. Consequently, the downpull coefficient can be regarded a function of (K_B) values which depended on gate geometry factors. Thus, the selection of gate lip shape should be treated as the basic criterion to control on the downpull and keep it

minimum as possible. However, the results of analysis indicate that, the minimum positive downpull may be obtained by adopting the inclined gate lip geometry with ($\theta = 35^o$), (shape No. 1) where their values of downpull coefficients range from (0.05 to 0.48), as shown in Fig. (15).

From the above results, a statistical model is built to establish an equation used to predict the (K_B) for any gate lip geometry depending on the available data, the following relationship was carried out as:

$K_B = f (x/d, e/d, Ys, Y/Yo, Re, V_j^2/2g, H_i)$

For high Reynolds number flow, (Re) has no strong effect on (K_B) so can be omitted.

The straightforward and applicable predicted formula indicated the effect of gate lip geometry was presented as:-

$$K_B = \left[-0.0022\left(\frac{H_i}{Ys}\right)^{-0.0793} - 0.2012\left(\frac{V_j^2/2g}{Ys}\right)^{0.1396} + 3.853(\theta)^{0.6335} - 0.2022\left(\frac{x}{d}\right)^{1.9089} - 0.7536\left(\frac{Y}{Yo}\right)^{0.0974} \right]$$ where (θ) is in radian.

This prediction is acceptable with good correlation coefficient equal to 0.942.

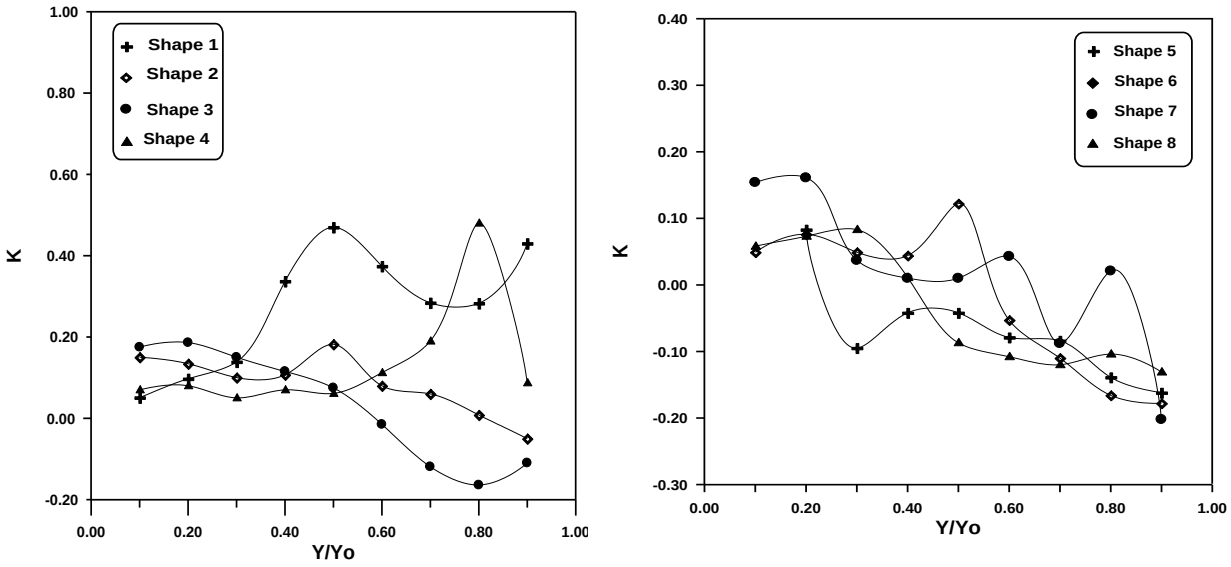

Figure (15):- Variation of the downpull Coefficients with Gate Openings for Different Gate geometry.

Conclusions

The two dimensional CFD modeling is used to solve a steady state incompressible Reynold-averaged Navier Stokes equations with (k-ε) turbulence closure model which is called as FLUENT program. The Reynols-averaged Navier Stokes equations are discretized using a control volume method and solved using the SIMPLE algorithm. Iterations proceed are continued until the sum of the normalized residuals is smaller than 10^{-3}.

A FLUENT program results are employed to estimate the downpull coefficient for nine gate lip geometries and from the results it can be concluded that:-

1- The variation of the gate opening (Y/Yo) has little effect on the values of top pressure coefficient (K_T) for a given gap width ratio ((b2/b1) = 0.2, 0.5, 1), whereas the gate geometry has no significant effect on the values of (K_T).

2- The bottom pressure coefficients have a main effect on the downpull which is influenced by the flow beneath the gate and the gate lip geometry.

3- The comparison between the results of inclined gate lip geometries with ($\theta = 35^o, 42^o, 45^o, 55^o$)

indicates that the use of inclined gate lip geometry with ($\theta = 35^o$) keeps the downpull coefficients as minimum positive values and reduces the effect of negative downpull.

4- It is indicated from the results of gate lip shapes with ($\theta = 45^o$ with e/d =0.42 and 0.64, $\theta = 42^o$ with e/d = 0.6, $\theta = 55^o$ with e/d = 0.2 and r/d = 1) that the negative downpull occurs at large opening ratio of (Y/Yo > 70%). The positive downpull values are obtained from using the inclined gate lip with ($\theta = 35^o, 55^o$).

5- A general statistical model is built to predict the values of (K_B) for any gate lip geometry.

References

- Aydin I., "Air Demand behind High Head Gates", Journal of Hydraulic Research, Vol. 40, No. 4, 2002.
- Ferzieger, J. L., and M. Peric, "Computational Methods for Fluid Dynamics", Springer-Verlag, Heidelberg, 1996.
- Cox Robert G., Ellis B. Pickell and W.P. Simmons, "Hydraulic Downpull on High head Gates", ASCE Discussion Hy. 5, May, 1960.
- Naudaschers E., Helmut E. Kobus and Ragam R. Rao, "Hydrodynamic Analysis for High head Leaf Gates", ASCE, Vol. 90, Hy. No. 3, 1964.
- Smith Peter M., and Jack M. Garrison "Hydraulic Downpull on Ice Harbor Power Gate", ASCE, Vol. 90, Hy. No. 3, 1964.
- Uppal , H. L. and Paul, T. C. "Design of Gates For High head Reservoir Outlets", Indian Journal of Power and River Valley Development , October , 1964.
- Murray, R. I. and Simmons, W. P., "Hydraulic Downpull Forces on Large Gates", A Water Resources Technical Publication, Report No.4, 1966.
- Narasimhan , S. and V. P., Bhargava "Flow-Induced Forces on Protruding Walls ", ASCE Discussion , Hy. No. 3, March, 1975.
- Sagar, B.T.A., "Downpull in High Head Gate Installation", Water Power and Dam Construction, March, April and May, 1977.
- Sagar, B.T.A., "Prediction of Gate Shaft Pressure in Tunnel Gate", Water Power and Dam Construction, March, 1978.
- Sager, B. T. A., "Downpull on High head Gates Installation", Water Power and Dam Construction, March, April and May, 1979.
- Thang, N. D. and Naudascher, E., "Approach Flow Effect on Downpull of Gates", ASCE, Vol. 109, No. Hy. 11, November, 1983.
- Naudascher, E. F., Palipu V. R., Andreas R., Patricio V. and Georg W., "Prediction and Control of Downpull on Tunnel Gates", ASCE, Vol.122. No. Hy. 5, May 1986.
- AL-Kadi , B. T., "Numerical Evaluation of Downpull Force in Tunnel Gates", Ph.D Thesis submitted to the College of Engineering , University of Baghdad , 1997.
- Ahmed, T. M., "Effect of Gate Lip Shapes on the Downpull Force in Tunnel Gates", Ph.D Thesis submitted to the College of Engineering , University of Baghdad , 1999.
- Sagar, B. T. A., "Gate Lip Hydraulics", Water Power and Dam Construction, March, 2000.
- Drobir H., Volker K. and Johannes S., "Downpull on Tunnel-Type High –Head Leaf Gates", IAHR/AIRH Hydraulic Report, Balkema, Rotterdam, 2001.
- Naudaschers E., "Hydrodynamic Forces", IAHR, Structure Design Manual, International Association of Hydro Research, Stockholm, Sweden, 1991.
- Andrade, J. L. and Amorim J. C., "Analysis of the Hydrodynamic Forces on Hydraulic Flood Gates", AIAA Journal, Vol.21, No. 10, 2003.
- Fluent User's Manual, Version 6.1, FLUENT Incorporated, Lebanon, N. H., 2003.
- Douglas, J. F. and Matthews, R. D., "Solving Problems in Fluid Mechanics", Longman Group Limited, 1996.
- Hoffmann, K. A., "Computational Fluid Dynamics for Engineers", The University of Texas in Austin, 1989.
- Reynolds, A. J., "Turbulent Flow in Engineering", John Wiley & Sons. 1974.